Control of chaos in noisy flows

Steven R. Bishop and Daolin Xu

Centre for Nonlinear Dynamics and Its Applications, University College London, Gower Street,
London WC1E 6BT, United Kingdom

A nonlinear dynamical system in a chaotic state is very sensitive to errors. Inherent noise in physical systems gives rise to difficulties for stabilizing chaotic systems onto desired unstable periodic orbits, particularly with large eigenvalues. The idea of adjusting the system state more frequently to eliminate error deviations from a desired orbit is utilized and given in variational form for flows. This control scheme acting on multiple sections can cope with relatively large noise levels. A Duffing oscillator and a parametrically excited pendulum are used in numerical studies. The relationship between controllable noise levels and the number of control sections is discussed. [S1063-651X(96)05409-8]

I. INTRODUCTION

The control of chaos has attracted much attention following the seminal article of Ott, Grebogi, and Yorke (OGY) [1]. This method has the ability to stabilize a desired orbit chosen from the many unstable periodic orbits coexisting with a chaotic attractor, without changing the global configuration of the system, which makes the OGY method different from previous methods [2–4]. In recent years, a number of different methods have been developed [5–18] motivated by the OGY method, many of which have been physically implemented; e.g., for driven beams [19], lasers [20,21], electronic circuits [22], chemical reactions [23], communications [24], and even for biological systems [25,26].

A nonlinear system in the chaotic state is very sensitive to initial conditions, particularly in chaotic systems with large Lyapunov exponents, see [14,17], such that a tiny error may lead to failure of a control process with errors amplified exponentially with time. Linearization of a nonlinear system in control, inaccuracy of experimental measurement, and a noisy environment all introduce errors into a control process. Considering the stabilization of an unstable periodic orbit embedded within an attractor, the growth, given by $e(\tau)$, of an error $e(0)$ to the unstable periodic orbit is dominated by the unstable eigenvalues λ_u of the orbit and the time τ, i.e.,

$$e(\tau) \sim e(0) \exp(\lambda_u \tau). \tag{1}$$

Figure 1 demonstrates a numerical example of the expansion of an error near an unstable periodic orbit in a parametrically excited pendulum [14]. Here $e(\tau)$ is defined by a distance from the unstable periodic orbit. The numerical computation shows that the error $e(\tau)$, at the time $\tau = 3 \times 2\pi$, is about 160 times larger than the initial error $e(0) = 0.01$ in only one recurrent time T (within which an orbit starts from an initial point and returns back to the same point, here $T = 3 \times 2\pi$) of the unstable period-3 orbit. This feature of rapid enlargement of errors in chaotic systems gives rise to additional difficulties during control.

A number of present methods [1,5,6,9–16] modify control parameters *once* each Poincaré return time. For the control of systems with large Lyapunov exponent or high-order

unstable periodic orbits, tiny errors introduced may ''kick'' the system state out of its controllable region. Therefore, the key observation is that the control interval must be reduced to decrease the time for errors to grow. Thus control must be more frequently applied to adjust the system state eliminating error deviations from a desired orbit before the errors grow too large. This idea was first used in the control of chaos by Hübinger *et al.* [18]. Here this idea is linked with a one-step optimal control scheme [11] and given in a variational form. The relationship between the number of control sections and controllable noise levels is investigated.

II. CONTROL ON MULTIPLE SECTIONS

In general, a continuous-time nonlinear dynamical system may be written as

$$\dot{\mathbf{x}} = \mathbf{f}(\mathbf{x}, \mathbf{p}), \quad \mathbf{x} \in \mathbf{R}^n, \quad \mathbf{p} \in \mathbf{R}^m, \tag{2}$$

where $\mathbf{x}$ is a vector of state variables and $\mathbf{p}$ a set of the parameters, such that at setting $\mathbf{p} = \mathbf{p}^*$, the system (2) undergoes a chaotic motion. There are typically an infinite number of unstable periodic orbits embedded within the chaotic motion [1]. An unstable periodic orbit satisfies $\mathbf{x}^*(t) = \mathbf{x}^*(t+T)$, where T is a recurrent period of the orbit. The motivation here is that $\mathbf{x}^*(t)$ can be viewed as an unstable period-K orbit having K fixed points ξ_k^* ($k = 1,2,\ldots K$) in the space $\Sigma_K \Gamma^{(k)} \in \Pi$. Here $\Gamma^{(k)}$ is one of the ''stroboscopic'' sections sampled in the phase space Π with a τ time interval; see Fig. 2(a). Thus the following relations must hold:

$$\xi_k^* = \mathbf{x}^*(t), \quad t = t_0 + k\tau, \quad k = 1,2,\ldots K, \quad K\tau = T, \tag{3}$$

where $\xi_k^* \in \Gamma^{(k)}$ and $\mathbf{x}^*(t) \notin \Gamma^{(k)}$ for $t \neq t_0 + k\tau$, and t_0 is initial time; see Fig. 2(b). In the full space Π, there exists a map $\mathbf{F}$ that satisfies the relations below for a K-periodic orbit,

$$\xi_{k+1}^* = \mathbf{F}(\xi_k^*, \mathbf{p}^*), \quad \xi_1^* = \mathbf{F}(\xi_K^*, \mathbf{p}^*) \tag{4}$$

and for any mapping point $\xi_i \in \Pi$,

$$\xi_{i+1} = \mathbf{F}(\xi_i, \mathbf{p}^*). \tag{5}$$
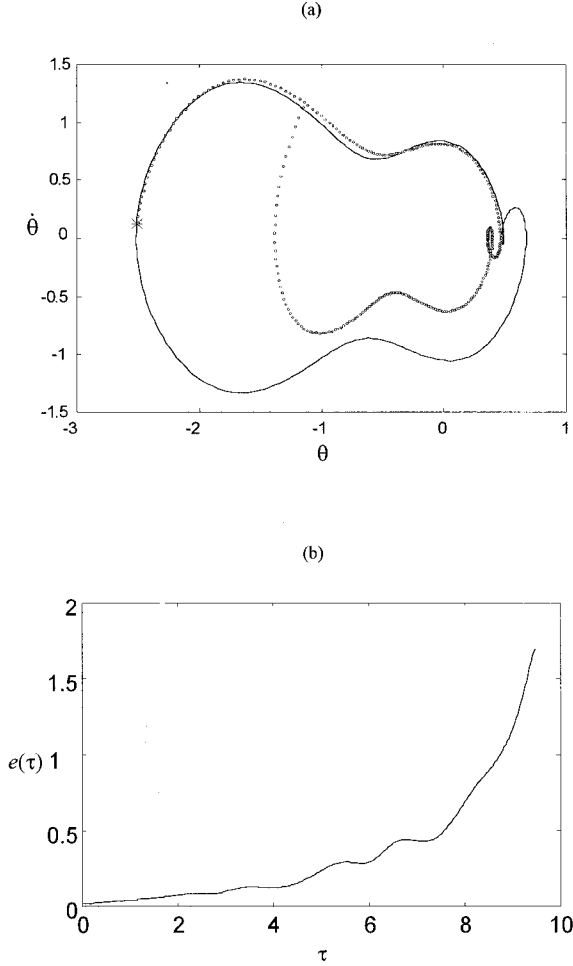

CONTROL OF CHAOS IN NOISY FLOWS

(a)

(b)

FIG. 1. A numerical example of an unstable oscillating period-3 orbit of a parametrically excited pendulum is illustrated. (a) The periodic orbit in the phase portrait starts from the initial point at $(-2.512\,660\,4, 0.065\,017\,1)$ marked by $*$. An error of $(0.01, 0.01)$ occurring at the initial point leads to a large deviation (dotted curve) from the unstable periodic orbit (solid curve). (b) The small error increases exponentially with time τ.

Let $\mathbf{x}(t;\mathbf{x}_0;\mathbf{p}^*)$ be a solution of (2) at time t with initial conditions $(t_0,\mathbf{x}_0,\mathbf{p}^*)$. Here ξ_i corresponds to the chaotic time series $\mathbf{x}(t;\mathbf{x}_0;\mathbf{p}^*)$ on the space Π. When ξ_i falls within a neighborhood Ω of one of the fixed points ξ_k^*, a one-step optimal control scheme [11] can be applied to stabilize ξ_{i+1} onto the fixed point ξ_{k+1}^* by perturbing the parameter $\mathbf{p}$ during the interval from i to $i+1$.

$$\delta\mathbf{p}_i = \alpha_k \delta\xi_i \quad (k=1,2,\ldots,K),$$

$$\delta\xi_i = \xi_i - \xi_k^*,$$

$$\alpha_k = -(D_\mathbf{p}^T\mathbf{F}(\xi_k^*,\mathbf{p}^*)\mathbf{D_p}\mathbf{F}(\xi_k^*,\mathbf{p}^*))^{-1}\mathbf{D_p}^T\mathbf{F}(\xi_k^*,\mathbf{p}^*)$$

$$\times \mathbf{D}_\xi\mathbf{F}(\xi_k^*,\mathbf{p}^*), \qquad (6)$$

where $\mathbf{D}_\xi\mathbf{F}(\xi_k^*,\mathbf{p}^*)$ is the Jacobian of the Poincaré map $\mathbf{F}$, and $\mathbf{D_p}^T\mathbf{F}(\xi_k^*,\mathbf{p}^*)$ denotes the differential of the map $\mathbf{F}$ with respect to the parameter $\mathbf{p}$. The superscript T denotes the transpose of a matrix as usual.

To apply (6), a variational method can be used to compute the discrete-time series ξ_i, $\xi_i \in \Pi$, the map $\mathbf{F}(\xi_i)$, the Jacobian $\mathbf{D}_\xi\mathbf{F}(\xi_k^*,\mathbf{p}^*)$, and the matrix $\mathbf{D_p}\mathbf{F}(\xi_k^*,\mathbf{p}^*)$. Let $\mathbf{x}(t;\mathbf{x}_0;\mathbf{p}^*)$ be a solution of (2) so that

$$\dot{\mathbf{x}}(t;\mathbf{x}_0;\mathbf{p}) = \mathbf{f}(\mathbf{x}(t;\mathbf{x}_0;\mathbf{p}^*),\mathbf{p}^*), \quad \mathbf{x}(t_0;\mathbf{x}_0;\mathbf{p}^*) = \mathbf{x}_0. \quad (7)$$

Differentiate (7) with respect to $\mathbf{x}_0$ to obtain

$$\mathbf{D_{x_0}}\dot{\mathbf{x}}(t;\mathbf{x}_0;\mathbf{p}^*) = \mathbf{D_x}\mathbf{f}(\mathbf{x}(t;\mathbf{x}_0;\mathbf{p}^*),\mathbf{p}^*)\mathbf{D_{x_0}}\mathbf{x}(t;\mathbf{x}_0;\mathbf{p}^*),$$

$$\mathbf{D_{x_0}}\mathbf{x}(t_0;\mathbf{x}_0;\mathbf{p}^*) = \mathbf{I}. \qquad (8)$$

Let $\mathbf{X}(t;\mathbf{x}_0;\mathbf{p}^*) = \mathbf{D}_{x_0}\mathbf{x}(t;\mathbf{x}_0;\mathbf{p}^*)$ and $\mathbf{f}(\mathbf{x},\mathbf{p}^*)$ denote $\mathbf{f}(\mathbf{x}(t;\mathbf{x}_0;\mathbf{p}^*),\mathbf{p}^*)$ then Eq. (8) becomes

$$\dot{\mathbf{X}}(t;\mathbf{x}_0;\mathbf{p}^*) = \mathbf{D}_x\mathbf{f}(\mathbf{x},\mathbf{p}^*)\mathbf{X}(t;\mathbf{x}_0;\mathbf{p}^*), \quad \mathbf{X}(t_0;\mathbf{x}_0;\mathbf{p}^*) = \mathbf{I}. \tag{9}$$

Differentiate (7) with respect to $\mathbf{p}^*$ to obtain

$$\mathbf{D_{p*}}\dot{\mathbf{x}}(t;\mathbf{x}_0;\mathbf{p}^*) = \mathbf{D_x}\mathbf{f}(\mathbf{x}(t;\mathbf{x}_0;\mathbf{p}^*),\mathbf{p}^*)\mathbf{D_{p*}}\mathbf{x}(t;\mathbf{x}_0;\mathbf{p}^*)$$

$$+ \mathbf{D_p}\mathbf{f}(\mathbf{x}(t;\mathbf{x}_0;\mathbf{p}^*),\mathbf{p}^*) \qquad (10)$$

with the initial condition $\mathbf{D_{p*}}\mathbf{x}(t_0;\mathbf{x}_0;\mathbf{p}^*) = \mathbf{0}$. Let $\mathbf{U}(t;\mathbf{x}_0;\mathbf{p}^*) = \mathbf{D_{p*}}\mathbf{x}(t;\mathbf{x}_0;\mathbf{p}^*)$ so that

$$\mathbf{U}(t;\mathbf{x}_0;\mathbf{p}^*) = \mathbf{D_x}\mathbf{f}(\mathbf{x},\mathbf{p}^*)\mathbf{U}(t;\mathbf{x}_0;\mathbf{p}^*)$$

$$+ \mathbf{D_p}\mathbf{f}(\mathbf{x},\mathbf{p}^*), \quad \mathbf{U}(t_0;\mathbf{x}_0;\mathbf{p}^*) = 0. \quad (11)$$

Putting Eqs. (7), (9), and (11) together forms a set of coupled differential equations given by

$$\left\{\begin{array}{c} \dot{\mathbf{x}}(t;\mathbf{x}_0;\mathbf{p}^*) \\ \dot{\mathbf{X}}(t;\mathbf{x}_0;\mathbf{p}^*) \\ \dot{\mathbf{U}}(t;\mathbf{x}_0;\mathbf{p}^*) \end{array}\right\} = \left\{\begin{array}{c} \mathbf{f}(\mathbf{x},\mathbf{p}^*) \\ \mathbf{D_x}\mathbf{f}(\mathbf{x},\mathbf{p}^*)\mathbf{X}(t;\mathbf{x}_0;\mathbf{p}^*) \\ \mathbf{D_x}\mathbf{f}(\mathbf{x},\mathbf{p}^*)\mathbf{U}(t;\mathbf{x}_0;\mathbf{p}^*)+\mathbf{D_p}\mathbf{f}(\mathbf{x},\mathbf{p}^*) \end{array}\right\},$$

$$\left\{\begin{array}{c} \mathbf{x}(t_0;\mathbf{x}_0;\mathbf{p}^*) \\ \mathbf{X}(t_0;\mathbf{x}_0;\mathbf{p}^*) \\ \mathbf{U}(t_0;\mathbf{x}_0;\mathbf{p}^*) \end{array}\right\} = \left\{\begin{array}{c} \mathbf{x}_0 \\ \mathbf{I} \\ \mathbf{0} \end{array}\right\}. \qquad (12)$$

The continuous time series $\mathbf{x}(t;\mathbf{x}_0;\mathbf{p}^*)$, $\mathbf{X}(t;\mathbf{x}_0;\mathbf{p}^*)$, and $\mathbf{U}(t;\mathbf{x}_0;\mathbf{p}^*)$ can be calculated by integrating (12) from the initial condition $\mathbf{x}(t_0;\mathbf{x}_0;\mathbf{p}^*)=\mathbf{x}_0 \in \Pi$. Thus the mapping point ξ_i, map $\mathbf{F}(\xi_i,\mathbf{p}^*)$, Jacobian $\mathbf{D}_\xi\mathbf{F}(\xi_k^*,\mathbf{p}^*)$, and matrix $\mathbf{D_p}\mathbf{F}(\xi_k^*,\mathbf{p}^*)$. $\xi_i \in \Pi$, can be written as follows:

$$\xi_i = \mathbf{x}(i\tau;\mathbf{x}_0;\mathbf{p}^*), \qquad (13)$$

$$\mathbf{F}(\xi_i,\mathbf{p}^*) = \mathbf{x}(\tau;\xi_i;\mathbf{p}^*), \qquad (14)$$

$$\mathbf{D}_\xi\mathbf{F}(\xi_i,\mathbf{p}^*) = \mathbf{X}(\tau;\xi_i;\mathbf{p}^*), \qquad (15)$$

$$\mathbf{D_p}\mathbf{F}(\xi_i,\mathbf{p}^*) = \mathbf{U}(\tau;\xi_i;\mathbf{p}^*). \qquad (16)$$

When $\mathbf{x}_0 \in \mathbf{x}^*(t)$ and $\mathbf{x}_0 = \xi_1^* \in \Gamma^{(1)} \in \Pi$, then $\mathbf{x}_0 = \xi_1^*$ is a fixed point on the section $\Gamma^{(1)}$ such that the fixed points ξ_k^*, $\mathbf{F}(\xi_k^*,\mathbf{p}^*)$, $\mathbf{D}_\xi\mathbf{F}(\xi_k^*,\mathbf{p}^*)$, and $\mathbf{D_p}\mathbf{F}(\xi_k^*,\mathbf{p}^*)$ can, respectively, be determined by (13), (14), (15), and (16). In the numerical procedure, the coupled differential Eq. (12) is integrated with a τ interval from a fixed point ξ_k^* on the section
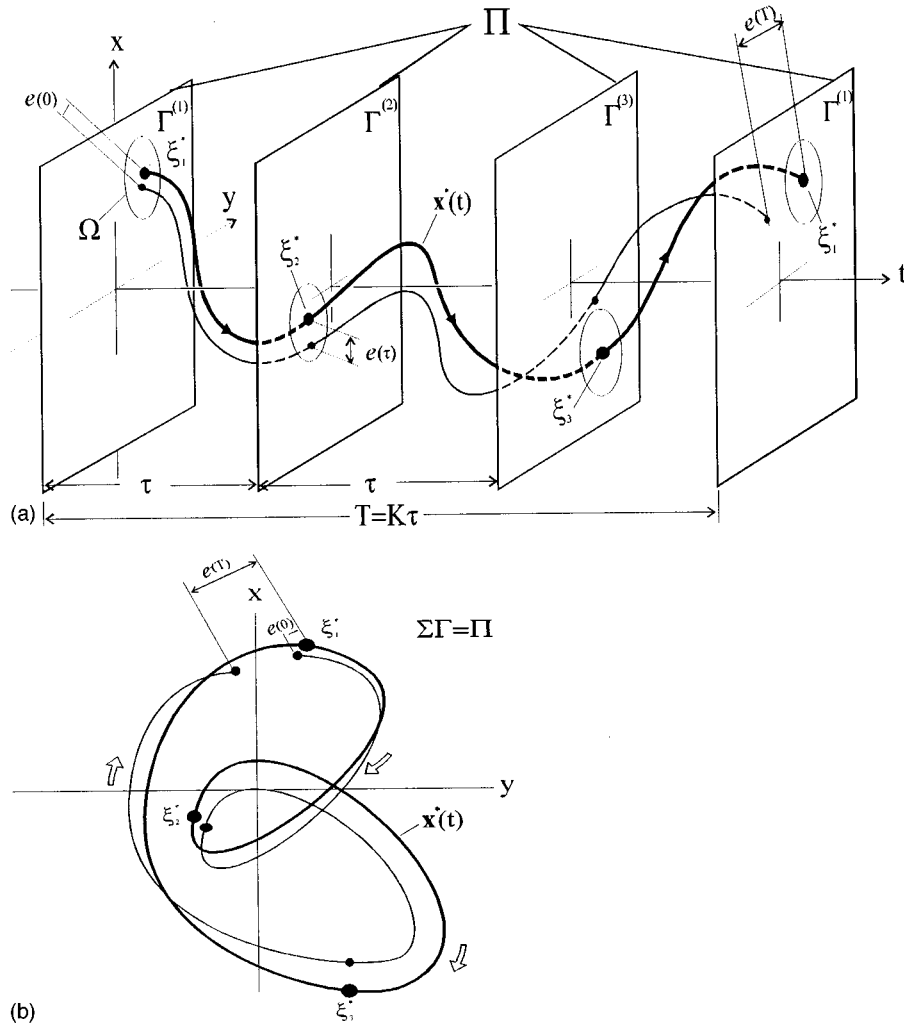
FIG. 2. Three "stroboscopic" sections set within a period T of an unstable periodic orbit $\mathbf{x}^*(t)$ with $\tau=T/3$. (a) The periodic orbit $\mathbf{x}^*(t)$ (thick curve) successively intersects the sections $\Gamma^{(k)}$ at points ξ_k^*, ($k=1,2,3$). Around ξ_k^*, a valid linearized region is marked by Ω. A small error $e(0)$ may cause a large deviation (denoted by the thin curve) from $\mathbf{x}^*(t)$ at $t=T$, where the $e(T)$ places the system state outside Ω, but not at $t=\tau$. (b) Three fixed points ξ_1^*, ξ_2^*, ξ_3^* in the phase space Π indicate a period-3 orbit in the sense of a period being τ.

$\Gamma^{(k)}$. After a τ interval of integration, the trajectory $\mathbf{x}(t;\xi_k^*;\mathbf{p}^*)$ intersects with the section $\Gamma^{(k+1)}$ at the fixed point ξ_{k+1}^* and the quantities in (14), (15), and (16) can be sequentially obtained. Therefore, the feedback control (6) can be applied at each τ interval on the space Π.

As the number of control sections K in (3) increase, the control time interval decreases within an orbit period T. Thus the variational algorithm can apply the perturbation $\delta\mathbf{p}$ more often (K times) than once each period T, such that the influence of the errors is diminished in each τ interval ($\tau < T$). A nontrivial benefit is that control input is renewed frequently to correct the state of the system onto a desired orbit $\mathbf{x}^*(t)$, resulting in an increase in the ability to stabilize highly unstable periodic orbits even in the presence of relatively large noise inputs.

III. NUMERICAL SIMULATIONS

To apply the new control scheme, the well-known Duffing oscillator is considered, which can be written in the form

$$\dot{x}=y,$$

$$\dot{y}=-cy+0.5x(1-x^2)+b\cos(\omega t),$$

$$\dot{t}=1. \qquad (17)$$

Figure 3 shows a chaotic attractor of the Duffing oscillator when parameters are set at $c=0.15$, $b=0.15$, and $\omega=0.8$. The mapping points are stroboscopically sampled at an interval of $2\pi/\omega$ (the driving period) from a single chaotic trajectory in phase space. An unstable period-5 orbit is indicated by five fixed points marked by the symbol $*$, which is embedded within the attractor. The forcing amplitude b is chosen as a control parameter.

In the absence of noise, a chaotic motion of the Duffing oscillator can be stabilized onto the unstable period-5 orbit (the unstable eigenvalue here is 23.3) by only setting one control section (i.e., $K=1$) in each recurrent time ($T=10\pi/\omega$) of this orbit. Figure 4 demonstrates the control process plotting the trajectory just before and just after the control in
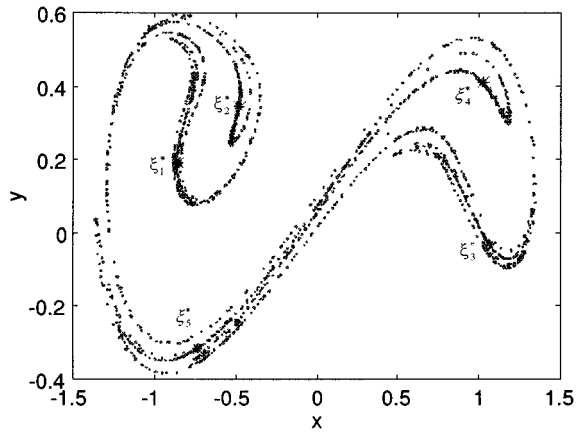
FIG. 3. A chaotic attractor of the Duffing oscillator described in Eq. (17), $c=0.15$, $b=0.15$, and $\omega=0.8$, is plotted by 2000 mapping points, which are stroboscopically sampled at intervals of $2\pi/\omega$ from a single chaotic trajectory in phase space. Five fixed points of an unstable period-5 orbit that is embedded within the attractor are indicated by the symbol *. The locations of the fixed points are $\xi_1^*=(-0.859\,167\,580,\ 0.192\,828\,460)$, $\xi_2^*=(-0.477\,363\,565,\ 0.345\,571\,833)$, $\xi_3^*=(1.063\,321\,87,\ -0.032\,301\,406\,9)$, $\xi_4^*=(1.027\,517\,16,\ 0.409\,679\,492)$, $\xi_5^*=(-0.729\,448\,553,\ -0.316\,140\,592)$.

x and y against t. The stabilized system state follows the unstable period-5 orbit that can be viewed in the phase portrait; see Fig. 4(c).

To examine the efficiency of the new control scheme, first we consider a simple case regarding the effect of a constant error. A typical example is carried out to show the relationship between the maximum controllable error and the number K of control sections in the stabilization of the unstable period-5 orbit; see Fig. 5. For simplicity, here an error is added only to the variable y once every recurrent time $T=10\pi/\omega$ of the periodic orbit. For the chosen number of sections K, we increase the value of the error until the control fails, giving the maximum controllable error. In Fig. 5, the maximum controllable errors are indicated by the point ○ corresponding to the number of control sections as K is varied. As can be seen, for $K=1$, the maximum controllable error was found to be 0.0008. Initially the ability to cope with errors in the control is enhanced as the number K of control sections increases. After $K=6$, the curve tends to flatten off and the maximum controllable error is up to about 0.26 in this specific stabilization. The one-step optimal scheme [11] is based on linearization, and consequently the error at this level may place the system state on the margin of the valid linearized neighborhood of the orbit. In this context, a further increase in the number of control sections will achieve no benefit. The maximal controllable error is restricted by the size of the linearized neighborhood of the orbit.

To further illustrate the effectiveness of control on multiple sections, we investigate a complicated situation of control in the presence of noise. Assume that noise is acting like a sequence of impulses whose amplitude and impulse frequency are both normally distributed. A time series of noise will thus be input into the variables x and y at irregular intervals. We will study the case of stabilizing a chaotic state
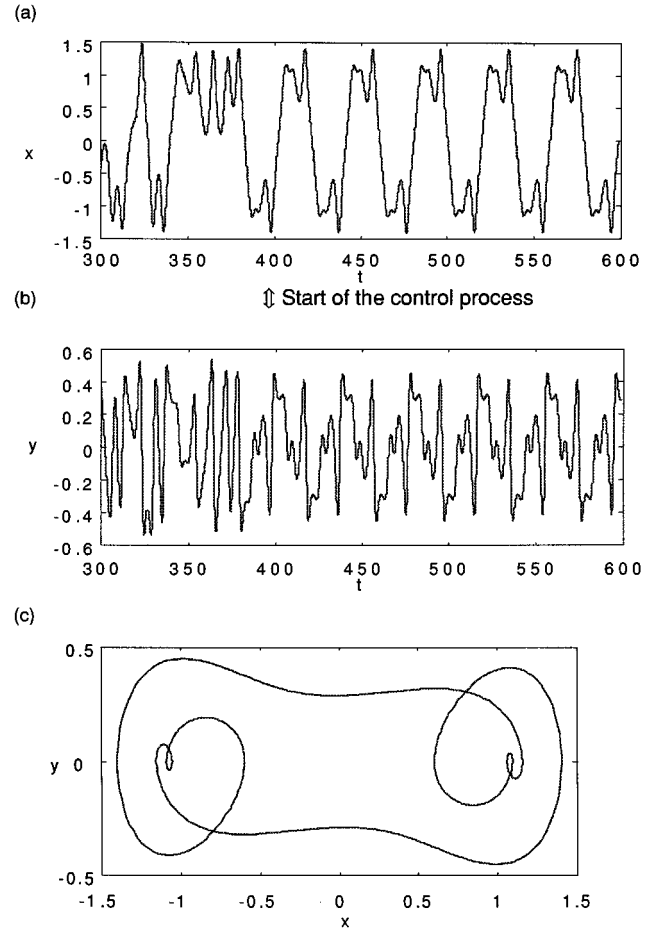

FIG. 4. A chaotic motion of the Duffing oscillator is stabilized onto the unstable period-5 orbit (with unstable eigenvalue 23.3) after $t=392$. The stabilization is carried out in the absence of noise using control once (i.e., $K=1$) in each recurrent time $(10\pi/\omega)$ of this orbit. (a) The controlled trajectory in x against t; (b) the controlled trajectory in y against t; (c) the phase portrait of the unstable period-5 orbit.
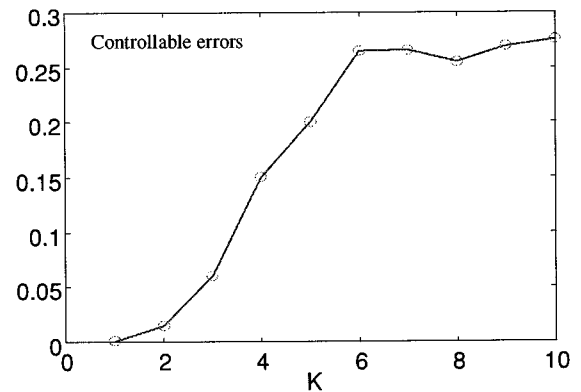

FIG. 5. An example of the relationship between the controllable errors and the number K of control-sections in the stabilization of an unstable period-5 orbit. The symbol ○ indicates the maximum controllable error corresponding to the number of K of control sections.
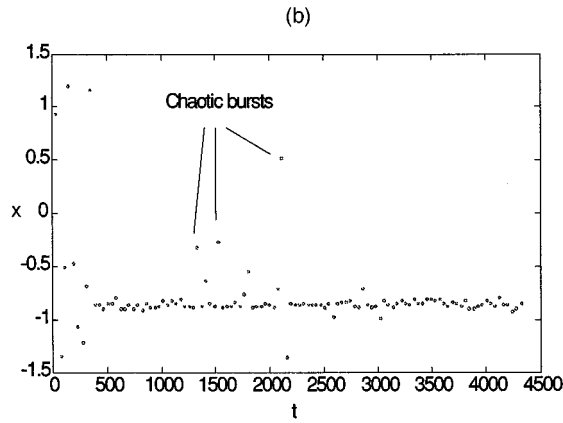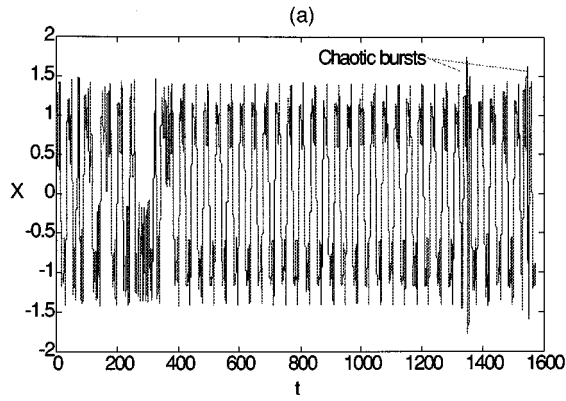
(a)

(b)

FIG. 6. Stabilization of the chaotic motion of the Duffing oscillator onto an unstable period-5 orbit in the presence of noise using five control sections ($K=5$). The control is switched on after $t=392$. (a) In the time series of the variable x, the chaotic trajectory is stabilized onto the periodic orbit, but the control is unsuccessful at $t=1350$ and $t=1520$, where the system state is "kicked" by the noise off the periodic state into the chaotic state. (b) A mapping of the variable x sampled each recurrent time ($10\pi/\omega$) of the periodic orbit shows a longer time scale of the control process. The dense points along the horizontal indicate that the system state stays on the periodic orbit. During $t=1350$–2200 the separated mapping points apart from the dense points indicate bursts of chaotic motions.

onto the unstable period-5 orbit. The system state is disturbed by noise to the level of approximately 7% of the size of the periodic orbit (the maximum amplitude of noise is bounded in x within 0.1 and in y within 0.033).

For such levels of noise, the stabilization, in general, fails when $K<5$. Figure 6(a) shows the case ($K=5$) in which the control is switched on after $t=392$, and the chaotic trajectory is stabilized onto the period-5 orbit, but the control is unsuccessful at $t=1350$ and $t=1520$, where the system state moves off from the periodic state into the chaotic state. A mapping series of the variable x sampled each recurrent time ($10\pi/\omega$) shows a longer time scale of the control process in Fig. 6(b). The dense points lining up along the horizontal axis indicate that the system state stays on the periodic orbit. However, the control loses robustness somewhere during $t=1350$–2200 in which the mapping points separated from the dense point line indicate bursts of chaotic motion. Con-
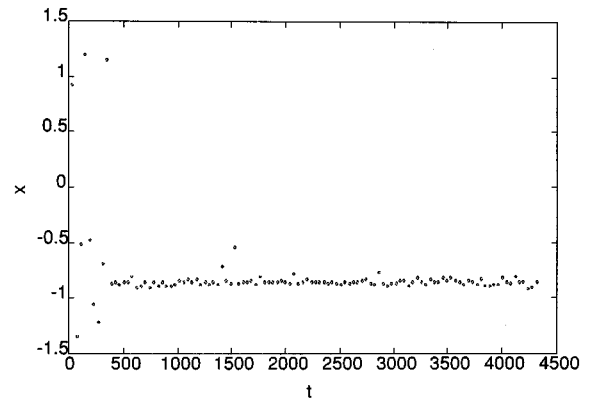

FIG. 7. Stabilization of the chaotic motion of the Duffing oscillator onto a unstable period-5 orbit in the presence of noise using 12 control sections ($K=12$). The control is switched on after $t=392$. A mapping of the variable x sampled each recurrent time ($10\pi/\omega$) of the periodic orbit shows a successful control process. The dense points parallel to the horizontal axis indicate that the system state stays close to the periodic orbit.

trol using the setting $K=5$ cannot suppress chaos completely since the noise impulses can still move the system state away from the stabilized periodic orbit at some time.

Using the same conditions as above, but with the setting changed to $K=12$, the system state is stabilized onto the period-5 orbit successfully, see Fig. 7, without significant chaotic bursts. In numerical simulations, the cases of $K=6$, 7, 8, 9, and 10 were also tried, indicating that chaotic bursts cannot be completely excluded but decrease as K increases.

The new method has also been applied to the parametrically excited pendulum described by

$$\ddot{\theta}+c\dot{\theta}+(1+p\cos\omega t)\sin\theta=0. \qquad (18)$$

When the parameters are set at $c=0.1$, $p=2$, and $\omega=2$, the system behaves chaotically with many unstable periodic orbits embedded within the chaotic motion; some possess large eigenvalues (100's, 1000's); see [14]. Here the parameter ω is used as a control parameter.
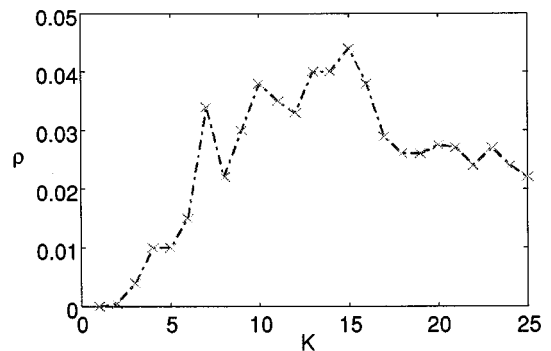

FIG. 8. The relationship between ρ (the controllable noise level) and K (the number of control sections) with the restriction of the parameter perturbation set at $|\delta\omega|<0.5$. This result is based on the control of the period-4 orbit of the parametrically excited pendulum, where the points (marked by the symbol $\times$) indicate the maximum controllable noise levels.
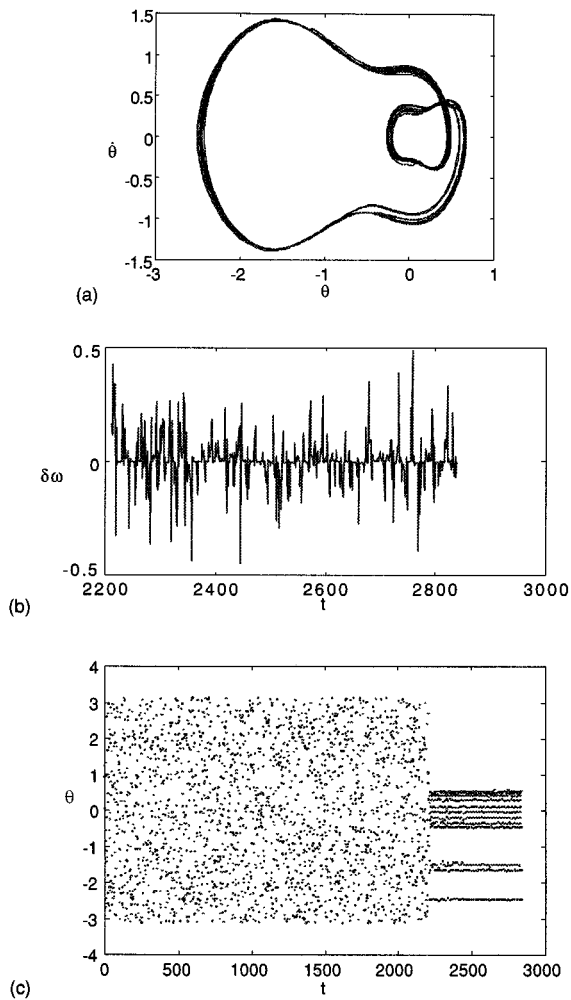
(a)

(b)

(c)

FIG. 9. (a) The phase portrait of the controlled period-4 orbit whose largest eigenvalue (in magnitude) is -562.3, which is "fuzzy" due to the effects of noise with ($K=12$, $\rho=0.03$, $|\delta\omega| <0.5$); (b) the parameter perturbations required to stabilize the periodic orbit; (c) the mapping points on 12 control sections.

In the presence of noise, which is added to both variables (the angular θ and the angular velocity $\dot{\theta}$), the stabilization of an oscillating unstable period-4 orbit, whose largest amplitude of the eigenvalue is -562.3, is investigated. A relationship between the controllable noise levels ρ and the number K of control sections is shown in Fig. 8. The points marked by $\times$ joined by lines indicate the maximum controllable noise levels corresponding to the number of sections K. In all simulations, the initial condition of the system state is the same starting from the point $(-2.474\ 21, 0.085\ 205)$ and the

parameter perturbation is bounded $|\delta\omega|<0.5$, which will be set to zero if $|\delta\omega|$ exceeds this value. As can be seen, when $K=1$, the controllable noise level ρ is less than 0.0001, $K=2$, $\rho=0.0005$, $K=3$, $\rho=0.004$, and so on. For the orbit described, the highest noise level $\rho=0.044$ can be controlled with $K=15$, which is about four times that of the achievable level for $K=4$. Selecting the proper number of control sections can greatly enhance the ability to cope with noise. Note that the controllable noise level, in general, decreases as the number of sections increases after $K=15$. One possible reason is that when the number of sections increases, the time for control is shortened, while directing a trajectory onto the desired orbit requires larger perturbations if the time interval for control is less. When the required perturbation exceeds its bounded value, the perturbation will be set to zero (which is not the required quantity for the correct control). Thus incorrect control inputs may result in failure of the control at certain levels of noise. In other numerical studies (not reported here), the pattern of this relationship between ρ and K is roughly similar when the perturbation is limited to $|\delta\omega| <1.0$, but the controllable noise level is higher. Using different segments of a noise time series (but with the same level) produces some differences, but the relationship between ρ and K remains qualitatively similar.

In Fig. 9, an example of stabilizing the unstable period-4 orbit is shown where the noise level ρ is 0.03, using 12 control sections ($K=12$) with a restriction on the perturbations of $|\delta\omega|<0.5$. In the phase space, the orbit is "fuzzy" due to the effects of noise, see Fig. 9(a). Figure 9(b) demonstrates the required parameter perturbations, which is renewed every control interval $\tau=\pi/3$. The orbit is sampled on the 12 control sections and the mapping points are plotted in Fig. 9(c), which indicates a longer time scale for the stabilization.

IV. CONCLUSION

In chaotic systems, an error can be expanded at an exponential rate with time such that small errors or noise inputs can easily affect a control process of stabilizing unstable periodic orbits. The idea of reducing the time for errors to grow by increasing control sections is powerful to cope with this issue, particularly when the orbits possess large eigenvalues. This paper links the concept of multiple sections with the one-step optimal scheme [11] given in a variational formulation applicable to flows. The relationship between the number of control sections and controllable noise levels is investigated. Numerical simulations show that the proposed scheme can significantly enhance the ability to cope with noise in the stabilization of unstable periodic orbits, even those that have large eigenvalues.

[1] E. Ott, C. Grebogi, and J. A. Yorke, Phys. Rev. Lett. **64**, 1196 (1990).

[2] A. W. Hübler, Helv. Phys. Acta **62**, 343 (1989).

[3] E. A. Jackson and A. W. Hübler, Physica D **44**, 407 (1990).

[4] R. Lima and M. Pettini, Phys. Rev. A **41**, 726 (1990).

[5] G. Nitsche and U. Dressler, Physica D **58**, 153 (1992).

[6] V. Petrov, B. Peng, and K. Showalter, J. Chem. Phys. **96**, 7506 (1992).

[7] K. Pyragas, Phys. Lett. A **170**, 421 (1992).

[8] S. Bielawski, D. Derozier, and P. Glorieux, Phys. Rev. E **49**, 971 (1994).

[9] M. A. Matias and J. Guemez, Phys. Rev. Lett. **72**, 1455 (1994).

[10] Z. Toroczkai, Phys. Lett. A **190**, 71 (1994).

[11] S. R. Bishop and D. Xu, in *Proceedings of the Tenth International Conference on Systems Engineering,* edited by K. Burnham and G. James (University of Coventry, Coventry, 1994), Vol. 1, pp. 95–102.

[12] D. Xu and S. R. Bishop, Chaos Solitons Fractals **4**, 1931 (1994).

[13] D. Xu and S. R. Bishop, Phys. Lett. A **210**, 273 (1996).

[14] S. R. Bishop, D. Xu, and M. J. Clifford, Proc. R. Soc. London Ser. A (to be published).

[15] D. Xu and S. R. Bishop, Int. J. Bifurc. Chaos **5**, 1741 (1995).

[16] S. R. Bishop and D. Xu, J. Sound Vib. (to be published).

[17] B. Hübinger, R. Doerner, W. Martienssen, M. Herdering, R. Pitka, and U. Dressler, Phys. Rev. E **50**, 932 (1994).

[18] B. Hübinger, R. Doerner, and W. Martienssen, Z. Phys. B **90**, 103 (1993).

[19] W. L. Ditto, S. N. Rauseo, and M. L. Spano, Phys. Rev. Lett. **65**, 3211 (1990).

[20] R. Roy, T. W. Murphy, Jr., T. D. Maier, Z. Gill, and E. R. Hunt, Phys. Rev. Lett. **68**, 1259 (1992).

[21] R. Meucci, W. Gadomski, M. Ciofini, and F. T. Arecchi, Phys. Rev. E **29**, 2528 (1994).

[22] H. Dedieu and M. Ogorzalek, Int. J. Bifurc. Chaos **4**, 447 (1994).

[23] V. Petrov, V. Gaspar, J. Masere, and K. Showalter, Nature **361**, 240 (1993).

[24] S. Hayes, C. Grebogi, E. Ott, and A. Mark, Phys. Rev. Lett. **73**, 1781 (1994).

[25] A. Garfinkel, M. L. Spano, W. L. Ditto, and J. N. Weiss, Science **257**, 1230 (1992).

[26] S. J. Schiff, K. Jerger, D. H. Duong, T. Chang, M. L. Spano, and W. L. Ditto, Nature **370**, 615 (1994).